Trans. Japan Soc. Aero. Space Sci.
Vol. 46, No. 151, pp. 47–51, 2003

MEMS-Based Solid Propellant Rocket Array Thruster with Electrical Feedthroughs*

By Shuji TANAKA,[1)] Ryuichiro HOSOKAWA,[1)] Shin-ichiro TOKUDOME,[2)] Keiichi HORI,[2)] Hirobumi SAITO,[2)] Masashi WATANABE[3)] and Masayoshi ESASHI[4)]

[1)]*Department of Mechatronics and Precision Engineering, Tohoku University, Sendai, Japan*
[2)]*The Institute of Space and Astronautical Science, Sagamihara, Japan*
[3)]*Nichiyu Giken Kogyo Co., Ltd., Kawagoe, Japan*
[4)]*New Industry Creation Hatchery Center, Tohoku University, Sendai, Japan*

(Received June 27th, 2002)

The prototype of a solid propellant rocket array thruster for simple attitude control of a 10 kg class micro-spacecraft was completed and tested. The prototype has 10×10 $\phi 0.8$ mm solid propellant micro-rockets arrayed at a pitch of 1.2 mm on a 20×22 mm substrate. To realize such a dense array of micro-rockets, each ignition heater is powered from the backside of the thruster through an electrical feedthrough which passes along a propellant cylinder wall. Boron/potassium nitrate propellant (NAB) is used with/without lead rhodanide/potassium chlorate/nitrocellulose ignition aid (RK). Impulse thrust was measured by a pendulum method in air. Ignition required electric power of at least 3–4 W with RK and 4–6 W without RK. Measured impulse thrusts were from 2×10^{-5} Ns to 3×10^{-4} Ns after the calculation of compensation for air dumping.

Key Words: Micro-Thruster, Micro-Electromechanical System (MEMS), Solid Propulsion, Micro-Space Craft

1. Introduction

Spacecraft weight has increased approximately 5–10 times in the past 20 years. Launching a heavy spacecraft, however, requires a large rocket with sufficient payload, and the cost is enormous. These factors are especially severe for interplanetary or deep-space missions, where the spacecraft must escape from earth's gravity. In such missions, minimizing the risk of failures is one of the most important concerns, and this makes the development of spacecraft consume immense capital and time. Therefore, the application of spacecraft is severely limited for industrial and scientific purposes.

To reduce the cost of spacecraft and open up a new application area of space technology, miniaturizing spacecraft by applying micro-electromechanical system (MEMS) technology plays a key role. In 1995, the National Astronautics and Space Administration (NASA) of the U.S.A. implemented "New Millennium Program" to dramatically miniaturize spacecraft. The goals of this program include the development of micro-spacecraft with weight of about 10 kg or less. For such micro-spacecraft, most of their components, including thrusters for attitude control, should be miniaturized by applying MEMS technology.

Recently, several kinds of MEMS-based thrusters, such as cold gas jet thrusters,[1)] solid propellant rocket thrusters,[2,3)] vaporizing liquid thrusters[4,5)] and a bi-propellant rocket thruster,[6)] are under development. TRW has proposed a solid propellant array thruster, "Digital Micropropulsion Thruster."[2)] Is is composed of one-shot solid propellant micro-rockets arrayed on a substrate, allowing thrust to be controlled digitally. LAAS-CNRS, CNES and Lacroix-Ruggieri have also developed a similar thruster.[3)]

The solid propellant array thruster is well constructed using MEMS technology, which is advantageous in terms of the integration and batch production capabilities of many mechanical, electrical, optical and/or chemical elements. The advantages of the thruster are as follows: 1) The system is completed on a substrate and compact. 2) Solid propellant has no anxiousness of leakage, unlike gas or liquid propellants. 3) The thruster has no moving parts. 4) The system is highly redundant. These advantages make the thruster useful for the simple attitude control of a 1–10 kg class micro-spacecraft. Figure 1 shows a typical example of possible applications for "Penetrator." Penetrator is a 15 kg simple spacecraft, which will travel to the lunar surface from a mother ship, "LUNAR-A." This mission is under preparation by the Institute of Space and Astronautical Science (ISAS) of Japan.

2. Design and Structure

First, we consider fundamental requirements for the solid propellant rocket thruster, assuming that it is used for the attitude control of a 10 kg spacecraft like Penetrator. Penetrator needs 1 m/s velocity increment to turn its nose toward the lunar surface. The 1 m/s velocity increment of the 10 kg spacecraft is obtained from a total impulse thrust of 10 Ns. If

*Presented at 23rd International Symposium on Space Technology and Science (ISTS2002), May 29, 2002

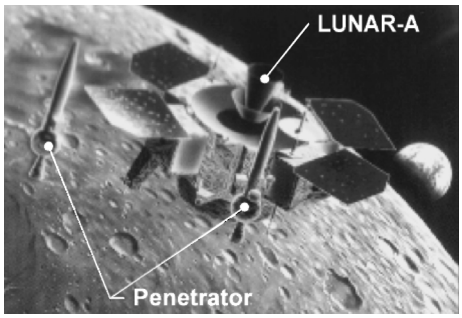

Fig. 1. Penetrator to be launched from LUNAR-A.

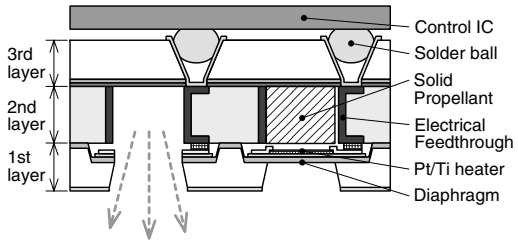

Fig. 2. Cross-sectional structure of a solid propellant rocket array thruster.

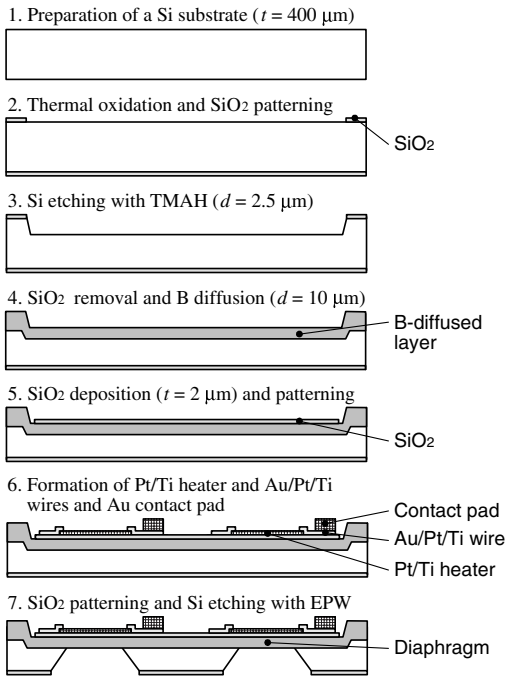

Fig. 3. Fabrication process of the third layer.

each micro-rocket on the thruster produces an impulse thrust of 1 mNs, the total impulse thrust of 10 Ns can be produced by 10,000 micro-rockets. If each micro-rocket occupies an area of 1 mm in diameter, the 100 × 100 array of micro-rockets (10,000 micro-rockets) requires an area of 10 × 10 cm. We think that this size is marginal, although further miniaturization is expected. Previous studies[2,3] only confirmed the preliminary concept of the thruster. In this paper, we propose a novel structure with electrical feedthroughs to ignition heaters for practical application.

Figure 2 illustrates the cross-sectional structure. The thruster consists of three layers. The first layer, a silicon layer, has nozzles and ignition heaters formed on diaphragms. The diaphragm, which bursts away after ignition, thermally insulates the ignition heater, and also seals the solid propellant. The second layer, a glass layer, holds the solid propellants and electrical feedthroughs which pass along propellant cylinder walls. The electrical feedthrough eliminates the need for wiring on the first layer, allowing the density of the micro-rocket array to be increased. The electrical feedthrough also enables the direct connection of a control circuit to the backside of the thruster. This reduces the size of the system and damage to the control circuit caused by exposure to cosmic rays.

3. Fabrication

The prototype has 10 × 10 ϕ0.8 mm solid propellant micro-rockets arrayed at a pitch of 1.2 mm on a 20 × 22 mm substrate. Figure 3 shows the fabrication process of the third layer. The process starts from preparing a 20 × 22 × 0.4 mm (100)-oriented silicon substrate (1 in Fig. 3). First, the silicon substrate is thermally oxidized, and the oxidized layer is patterned using buffered hydrofluoric acid (HF) solution to form mask openings (2). Through the mask openings, the silicon substrate is etched to a depth of 2.5 μm using tetramethyl ammonium hydroxide (TMAH) solution (3).

After removing the silicon dioxide (SiO_2) mask, boron is diffused for etch stop (4). Subsequently, a 2 μm thick SiO_2 film is deposited by plasma enhanced chemical vapor deposition (PECVD), and the SiO_2 film is patterned by buffered HF solution to form an electrical insulator (5). On it, platinum/titanium (Pt/Ti) ignition heaters and gold/platinum/titanium (Au/Pt/Ti) wires are formed using lift-off method. Additionally, gold electrical contact pads for connection to the second layer are formed on the Au/Pt/Ti wires (6). Finally, the backside SiO_2 film is patterned using buffered HF solution, and the silicon substrate is etched using ethylene diamine/pyrocatechol/water (EPW) to form nozzles and diaphragms (7). The array of the nozzles is shown on the left side in Fig. 6. The shape and expansion angle (70.5°) of the nozzle are defined by the crystal orientation of silicon.

Figure 4 shows the fabrication process of the second layer. A 1 mm thick Pyrex glass substrate is used as a starting material (1 in Fig. 4). First, a sputter-deposited chromium (Cr) mask is patterned (2), and the glass substrate is etched to a depth of 30 μm using buffered HF solution (3). After removing a photoresist film on the Cr mask, propellant cylinders with a diameter of 0.8 mm are formed by grinding using a high-speed milling machine (modified F-MACH 442, Toshiba Machine) (4). After the Cr mask is removed, nickel (Ni) is electroplated on a sputter-deposited Au/Cr seed layer (5), and then polished to damascene electrical contact pads

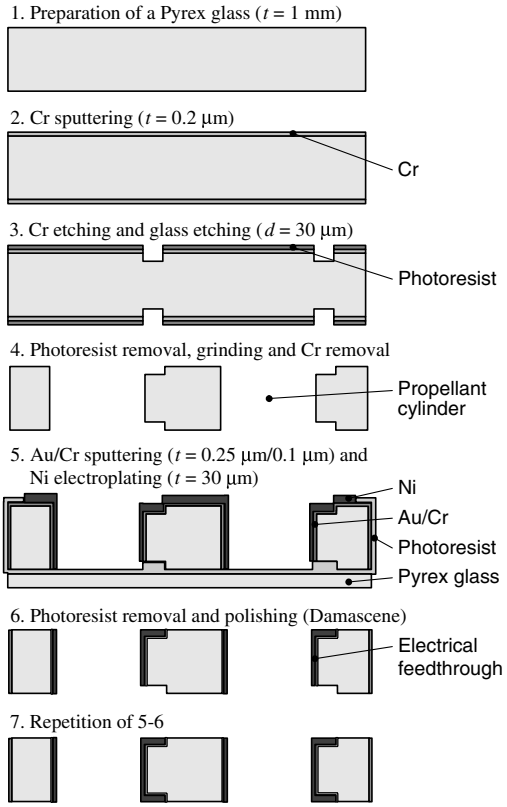

Fig. 4. Fabrication process of the second layer.

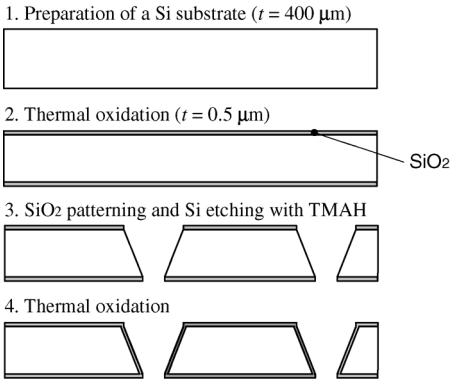

Fig. 5. Fabrication process of the first layer.

(6). The same processes are repeated on the opposite side (7).

Figure 5 shows the fabrication process of the first layer. A $20 \times 20 \times 0.4$ mm (100)-oriented silicon substrate is used as a starting material (1 in Fig. 5). First, the silicon substrate is thermally oxidized (2), and the oxidized layer is patterned using buffered HF solution to form mask openings. Using the SiO_2 mask, the silicon substrate is etched using TMAH solution to form through holes, and thin SiO_2 diaphragms at the bottom of the through holes are removed (3). Finally, the silicon substrate is thermally oxidized for electrical insulation (4).

The second and third layers are anodically bonded. The right micrograph in Fig. 6 shows the array of propellant

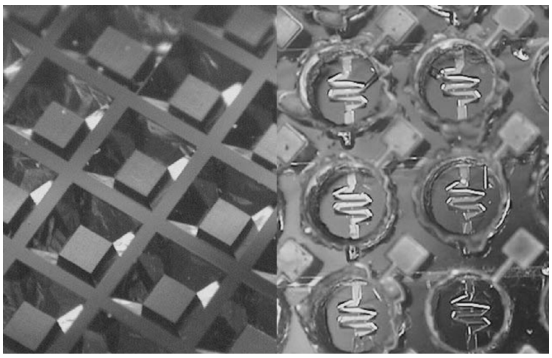

Fig. 6. Nozzles (left) and propellant cylinders with electrical feedthroughs (right).

cylinders without solid propellants. The ignition heaters on the diaphragms can be seen at the bottom of the propellant cylinders. In this study, we selected boron/potassium nitrate propellant (NAB) from several candidates including hydroxyl-terminated polybutadiene/ammonium perchlorate (HTPB/AP) and glycidyle azide polymer (GAP), because NAB has ignition capability at atmospheric pressure and low temperature. NAB slurry or a $\phi 0.8 \times 1$ mm NAB pellet shaped using a punch and die is inserted to the propellant cylinder. Lead rhodanide/potassium chlorate/nitrocellulose ignition aid (RK) is also used to fill the gap between the NAB pellet and the ignition heater. The end of the NAB pellet or the ignition heater is coated with liquid RK just before the NAB pellet or the NAB slurry is inserted into the propellant cylinder.

The first and second layers are bonded using adhesive. Subsequently, conductive epoxy is injected into the through holes on the first layer to create electrical contacts. In the future, solder balls will be inserted into the through holes, and a ball grid array (BGA) IC socket will be connected to the solder balls using the conductive epoxy.

4. Testing

First, we confirmed the performance of the ignition heater. Figure 7 shows the relationship between the electric power and temperature of the ignition heater. Epoxy resin was used as the replacement for solid propellant. We first measured the temperature of the ignition heaters without the epoxy resin using an infrared image microscope to confirm the relationship between the temperature and resistance of the ignition heater. Using this relationship, the temperature of the ignition heater covered with the epoxy resin was estimated. This estimation predicts that electric powers of about 3 W and 5 W are necessary to heat the ignition heater to 200°C and 500°C, which are the ignition temperatures of RK and NAB, respectively.

Next, we measured impulse thrust using a pendulum suspended in ambient air. Figure 8 shows an experimental setup. The thruster mounted on a printed circuit board is attached to the lower end of a balsa pendulum with a length of

Table 1. Summary of the test results.

No.	Propellant	Ignition power (W)	Ignition	Ignition delay (ms)	Combustion duration (ms)	Impulse thrust as measured (Ns)	Impulse thrust with air dumping compensation (Ns)
#1	NAB	5.9	Go	1000	66	1.1×10^{-4}	3.0×10^{-4}
#2	NAB	5.9	Go	208	62	1.9×10^{-5}	5.4×10^{-5}
#3	NAB	3.8	No-Go	—	—	—	—
#4	NAB + RK	3.8	Go	12	43	9.6×10^{-6}	2.2×10^{-5}
#5	NAB + RK	2.9	No-Go	—	—	—	—
#6	NAB + RK	3.6	Go	30	25	2.4×10^{-5}	3.0×10^{-5}
#7	NAB + RK	3.0	No-Go	—	—	—	—

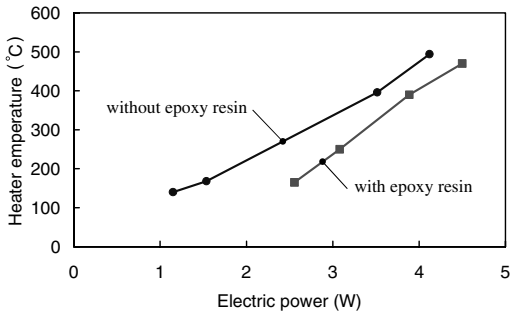

Fig. 7. Relationship between electric power and heater temperature.

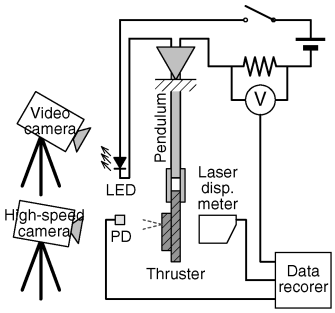

Fig. 8. Experimental setup for impulse thrust measurement in air.

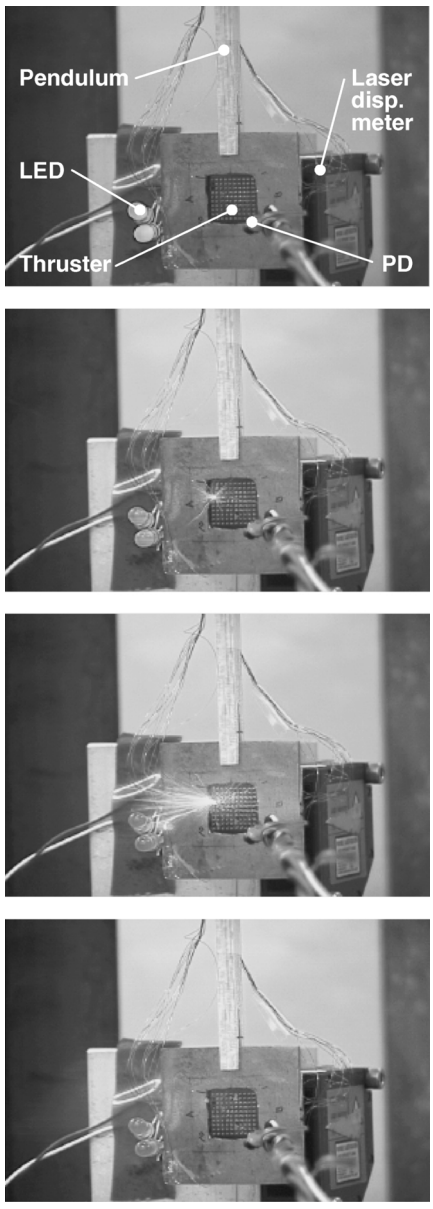

Fig. 9. Digital video images at ignition.

about 260 mm. Ignition signals are supplied using $\phi 100\,\mu$m copper wires led from the upper end of the pendulum. The motion of the thruster is measured using a laser displacement meter (Z4M-W40, OMRON). The ignition signal is visualized using a light emitting diode (LED), and light from the burning solid propellant is detected using a photodiode (PD). A high-speed camera with a frame rate of 500/s and a digital video camera are installed to record the action of the thruster.

Figure 9 shows digital video images at the time of ignition, and Table 1 summarizes the test results. Ignition delay and combustion duration were obtained from the records of the high-speed camera. These results confirmed that RK reduced ignition power and ignition delay, and reduced the energy required for ignition. The power required for igniting NAB and NAB with RK is approximately 4–6 W and 3–4 W, respectively, showing rough agreement with the estimation from Fig. 7.

Impulse thrust is calculated from the oscillation of the pendulum measured by the laser displacement meter. Figure 10 depicts the oscillation waveform measured in the test of No. 6. The oscillation waveform shows the influence of air dumping. Therefore, we use calculations to compensate

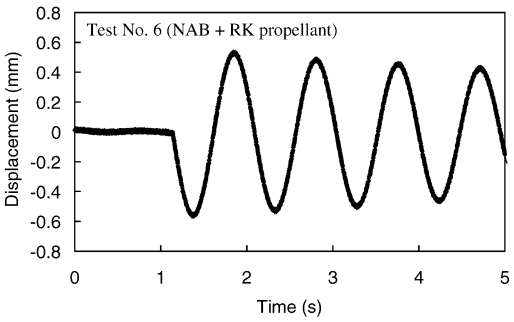

Fig. 10. Oscillation waveform measured in the test of No. 6.

the influence of air dumping. The motion of the pendulum follows

$$m\ddot{x} + mb\dot{x} + kx = 0, \tag{1}$$

where m is the mass of the pendulum, x is the displacement, b is the damping constant, and k is the spring constant. Equation (1) has a solution represented by

$$x(t) = e^{\lambda t}. \tag{2}$$

By substituting Eq. (2) into Eq. (1), λ is solved as follows:

$$\lambda = -\frac{b}{2} \pm \frac{\sqrt{4mk - m^2b^2}}{2m}i, \tag{3}$$

where the first term represents dumping, and the second term represents sine-wave oscillation. Thus, the amplitude of the oscillation is

$$x(t) = e^{-(b/2)t}. \tag{4}$$

The natural logarithm of Eq. (4) is

$$\ln x(t) = -\frac{b}{2}t. \tag{5}$$

We know $-b/2$ in Eq. (5) from oscillation waveforms like those in Fig. 10. Energy loss by air dumping in the first quarter period from ignition is given by

$$\int_{x(0)}^{x(\tau/4)} mb\dot{x}(t)\mathrm{d}x, \tag{6}$$

where τ is the oscillation period, and can also be determined from oscillation waveforms like those in Fig. 10.

Impulse thrusts with the compensation of air dumping by Eq. (6) are also shown in Table 1. The impulse thrusts range from 2×10^{-5} Ns to 3×10^{-4} Ns, showing considerable differences. Observation using the high-speed camera also confirmed considerable differences in the appearance of flames from the micro-rockets. Another problem is lower impulse thrust than the required value of 1 mNs, although the impulse thrust become higher under vacuum condition. We should reconsider the material and amount of solid propellant as well as the shape of the nozzles.

5. Conclusion

The prototype of a solid propellant rocket array thruster for the simple attitude control of a 10 kg class microspacecraft was completed and tested. The prototype has 10×10 ϕ0.8 mm solid propellant micro-rockets arrayed at a pitch of 1.2 mm on a 20×22 mm substrate. To realize such a dense array of micro-rockets, each ignition heater is powered from the backside of the thruster through an electrical feedthrough which passes along a propellant cylinder wall. Boron/potassium nitrate propellant (NAB) is used with/without lead rhodanide/potassium chlorate/nitrocellulose ignition aid (RK).

Impulse thrust was measured using a pendulum suspended in ambient air. Ignition required electric power of at least 3–4 W with RK, and 4–6 W without RK. The impulse thrusts were from 2×10^{-5} Ns to 3×10^{-4} Ns after calculating the compensation for air dumping. The impulse thrusts show considerable differences, and are lower than the required value of 1 mNs. Further study is necessary to optimize the material and amount of solid propellant as well as the shape of the nozzles.

Acknowledgments

This work was partly supported by the Ministry of Education, Culture, Sports, Science and Technology, Grant-in-Aid for Encouragement of Young Scientists, 12750808, 2000 and Grant-in-Aid for Exploratory Research, 14655077, 2002.

References

1) Köhler, J., Bejhed, J., Kratz, H., Bruhn, F., Lindberg, U., Hjort, K. and Stenmark, L.: A Hybrid Cold Gas Microthruster System for Spacecraftens. *Sensors Actuators A*, **97-98** (2002), pp. 587–598.
2) Lewis, D. H., Jr., Janson, S. W., Cohen, R. B. and Antonsson, E. K.: Digital Micropropulsion, *Sensors Actuators A*, **80** (2000), pp. 143–154.
3) Rossi, C., Orieux, S., Larangot, B., Do Conto, T. and Estève, D.: Design, Fabrication and Modeling of Solid Propellant Microrocket-Application to Micropropulsion, *Sensors Actuators A*, **99** (2002), pp. 125–133.
4) Mukerjee, E. V., Wallace, A. P., Yan, K. Y., Howard, D. W., Smith, R. L. and Collins, S. D.: Vaporizing Liquid Microthruster, *Sensors Actuators A*, **83** (2000), pp. 231–236.
5) Ye, X. Y., Tang, F., Ding, H. Q. and Zhou, Z. Y.: Study of a Vaporizing Water Micro-Thruster, *Sensors Actuators A*, **89** (2001), pp. 159–165.
6) London, A. P., Ayón, A. A., Epstein, A. H., Spearing, S. M., Harrison, T., Peles, Y. and Kerrebrock, J. L.: Microfabrication of a High Pressure Bipropellant Rocket Engine, *Sensors Actuators A*, **92** (2002), pp. 351–357.